Tensor renormalization group study of orientational ordering in simple models of adsorption monolayers

V. A. Gorbunov ⬤,[*] A. I. Uliankina ⬤, S. S. Akimenko, and A. V. Myshlyavtsev

Department of Chemistry and Chemical Engineering, Omsk State Technical University, 11 Mira Avenue, Omsk 644050, Russian Federation

A simple lattice model of the orientational ordering in organic adsorption layers that considers the directionality of intermolecular interactions is proposed. The symmetry and the number of rotational states of the adsorbed molecule are the main parameters of the model. The model takes into account both the isotropic and directional contributions to the molecule-molecule interaction potential. Using several special cases of this model, we have shown that the tensor renormalization group (TRG) approach can be successfully used for the analysis of orientational ordering in organic adsorption layers with directed intermolecular interactions. Adsorption isotherms, potential energy, and entropy have been calculated for the model adsorption layers differing in the molecule symmetry and the number of rotational states. The calculated thermodynamic characteristics show that entropy effects play a significant role in the self-assembly of dense phases of the molecular layers. All the results obtained with the TRG have been verified by the standard Monte Carlo method. The proposed model reproduces the main features of the phase behavior of the real adsorption layers of benzoic, terephthalic, and trimesic acids on a homogeneous surface of metal single crystals and graphite.

I. INTRODUCTION

Rational design of functional organic monolayers on solid surfaces with desired physicochemical properties has been an ongoing task over the past 20 years [1–5]. The structure of such a layer and its properties can be varied over a wide range by the appropriate choice of the size, shape, and chemical structure of the adsorbed molecules. However, the phase behavior of organic layers essentially depends on the experimental conditions: temperature, pressure, and density of the adsorption layer, and other factors. Today, reliable studies of organic adsorption layers rely on theoretical approaches and computer simulation methods [6–15].

A detailed theoretical description of an organic adsorption layer at the atomistic level often turns out to be laborious [14,16–19]. A possible solution to this problem is the coarse-grained lattice models [8,20–28]. Such models neglect the atomistic details of molecular layers, but they capture well the general patterns of their phase behavior. Any adequate model of an organic layer should consider the main features of the adsorption of functional organic molecules. The most important are (i) the large intrinsic size of the molecule compared to the period of the surface unit cell, (ii) orientational degrees of freedom of the adsorbed molecule, and (iii) the directionality and selectivity of intermolecular interactions in the layer. The latter is related to the chemical structure of the molecule and, as a rule, is expressed as dipole-dipole interactions and/or hydrogen bonding.

Lattice models of organic adsorption layers with different levels of dualization are usually studied by the Monte Carlo method. Other methods such as the transfer-matrix method or the tensor renormalization group (TRG) method are used much less [21,22,29,30]. However, the TRG has several advantages. The main feature is the direct calculation of the free energy of the model adsorption layer and subsequent direct thermodynamic analysis of its phase behavior. The result obtained with the TRG is purely thermodynamic since it corresponds to an infinite system. In addition, it is relatively simple to take into account directed and many-particle intermolecular interactions when constructing the tensor. Despite these advantages, today the TRG-based methods are mainly used to study only the simplest models of adsorption layers, such as the Langmuir model and adsorption models of hard-core particles of different sizes and shapes [30–34]. Most of these two-dimensional (2D) models do not allow for the rotation of the adsorbed molecule, as well as the directionality of intermolecular interactions. The simplest lattice models that consider orientational degrees of freedom or orientational states of the sites are the q-state "clock" model and the *XY* model as its generalization [35–38]. It has recently been shown that the TRG can also be successfully used to study orientational ordering in these magnetic models [39–44]. However, it is well known that any Ising-type model of magnets is equivalent to some lattice gas models [24,45,46]. Therefore, the features of the phase behavior observed in these magnetic models should also be expected in the models of adsorption layers. The Hamiltonian of the q-state clock model and the *XY* model as its generalization to continuous models is symmetric with respect to a simultaneous flip of both interacting spins (or orientable particles). There is no difference in direction for an interacting pair of particles in these models, but this is fundamentally important for the correct description of orientational ordering in

---
*Corresponding author: vitaly_gorbunov@mail.ru

adsorption layers consisting of functional organic molecules [22–24,46,47].

In this work, we propose a simple lattice model of the adsorption layer, which considers the rotation of the adsorbed molecule as well as the directionality of intermolecular interactions. The symmetry of the functional groups' arrangement in the adsorbed molecule and the amount of its rotational states are the model parameters. Within the framework of the proposed model, we have demonstrated that the TRG method can be successfully used for the analysis of orientational ordering in organic adsorption layers with directed intermolecular interactions.

II. MODEL

To describe the phase behavior of organic molecular layers on a solid surface one has to take into account the orientational degrees of freedom of the adsorbed molecule and directionality of intermolecular interactions. The mutual orientation of the interacting functional groups of neighboring molecules is crucial [22–24,46]. A well-known example of such short-range and highly directed interaction is hydrogen bonding [2,3].

Let us describe a simple lattice model, which generally takes into account both the short range and directionality of the interactions. Adsorption layers of benzoic, terephthalic, and trimesic acids are considered as prototypes. These molecules differ in the number and positions of the carboxyl (-COOH) groups capable of forming a hydrogen bond [3]. The molecule of benzoic acid has one -COOH group and belongs to C_1 symmetry, terephthalic acid has two -COOH groups and C_2 symmetry of their arrangement, and trimesic acid has three -COOH groups located at the angle of $120°$ relative to each other (C_3 symmetry). In the proposed model, an adsorbed molecule occupies one site on a triangular, square, or hexagonal lattice with the linear size equal to L sites. The lattice constant is assumed to be unit. Positions of the functional groups in the adsorbed molecule or the symmetry of the molecule are given by the c parameter (Fig. 1). The c parameter is equal to 1, 2, and 3 for benzoic, terephthalic, and trimesic acid molecules, respectively. This means that the molecule transforms into itself when rotating in plane relative to the molecule center by the angle of $2\pi/c$. The adsorbed molecule has n rotational states uniformly distributed around the angular diameter $[0, 2\pi/c]$. For example, the model adsorption layer of molecules with C_2 symmetry ($c = 2$) at $n = 3$ suggests that an adsorbed molecule has three different orientations uniformly distributed from 0 to π. In these orientational states, the angles between one of the functional groups of the adsorbed molecule and the lattice vector are 0, $\pi/3$, and $2\pi/3$. Thus, the total number of site states in the $c = 2$, $n = 3$ model is 4, including the empty (unoccupied) state. The origin of the orientation angle is determined by the state in which one of the functional groups of the adsorbed molecule coincides with one of the lattice vectors.

In the well-known atomistic potentials, a hydrogen bond potential is represented as the product of the radial and angular parts of the interaction [48–51]. The radial part is usually described by the Lennard-Jones 12-10 or exponent-6 poten-
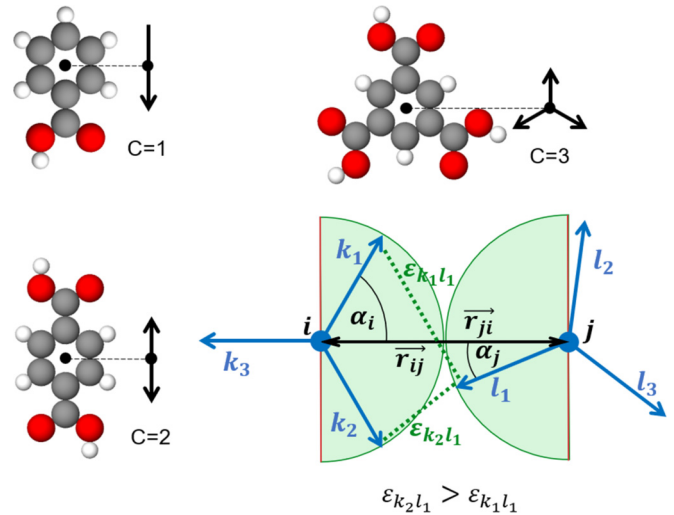

FIG. 1. Schematic representation of molecules with C_1, C_2, and C_3 symmetry: benzoic, terephthalic, and trimesic acids. In the lower right part of the figure, a pair of interacting "functional groups" is shown. Vector r_{ij} is directed from the lattice site i to the lattice site j (from the center of the molecule i to the center of the molecule j). The angles α_i and α_j determine the orientation of the molecules adsorbed on sites i and j with respect to the vectors r_{ij} and r_{ji}, correspondingly. The green semicircle demonstrates the favorable zone of interactions between i and j molecules; $\varepsilon_{k_1 l_1}$ and $\varepsilon_{k_2 l_1}$ are the interactions between the first and second functional group of the i molecule and first functional group of the j molecule, respectively.

tials. These are short-range interactions. Therefore, in our lattice model we consider only the interactions between the nearest neighbor molecules. The angular part is represented by the first, second, or fourth power of the cosine of the angle between the hydrogen donor, proton, and hydrogen acceptor. Obviously, this angle is determined by the mutual orientation of the functional groups of the interacting molecules. By analogy, we write an expression for the attractive interaction ε_{kl} between the functional groups of two neighboring molecules [Fig. 1 and Eq. (1)]:

$$\varepsilon_{kl} = 0, \text{ if } \cos\left(\alpha_i - \frac{2\pi k}{c}\right) \leqslant 0 \text{ or } \cos\left(\alpha_j - \frac{2\pi l}{c}\right) \leqslant 0$$

$$\varepsilon_{kl} = w\cos^2\left(\alpha_i - \frac{2\pi k}{c}\right)\cos^2\left(\alpha_j - \frac{2\pi l}{c}\right), \quad \text{otherwise,}$$

(1)

$$U_{ij} = \sum_{k=0}^{c-1}\sum_{l=0}^{c-1}\varepsilon_{kl}, \tag{2}$$

where $c=\{1, 2, 3, \dots\}$ is the parameter determined by the point symmetry of the functional organic molecule; k and l are the order numbers of functional groups of the interacting molecules. The orientation of the ith molecule (α_i) relative to the r_{ij} vector connecting the centers of the interacting molecules is given by the orientation of the zero functional group ($k = 0$). In the same way, the orientation of the jth molecule and its functional groups are determined by the α_j angle and order number of the functional group (l). When the directions of k and l functional groups of the neighboring molecules i and j coincide with the vector connecting their

centers, the interaction energy ε_{kl} of these functional groups is equal to $w < 0$. As is seen from Eq. (1), the energy ε_{kl} is either negative (attraction) or equal to zero. The total interaction energy U_{ij} between i and j molecules is the sum of the interaction energies ε_{kl} between each functional group of the ith molecule with each functional group of the jth molecule. Thus, both sums in Eq. (2) run over all the functional groups of the interacting molecules.

It is also possible to include in the model the energy $\Delta > 0$ of isotropic repulsive interactions. In the first approximation, it considers the intrinsic size of the neighboring molecules. Thus, the total interaction potential of a pair of molecules adsorbed on neighboring lattice sites is equal to

$$U_{ij} = \Delta + \sum_{k=0}^{c-1} \sum_{l=0}^{c-1} \varepsilon_{kl}. \tag{3}$$

The thermodynamic Hamiltonian of the model for an open thermodynamic system can be written as follows,

$$\mathcal{H} = \sum_{\langle i,j \rangle} U_{ij} n_i n_j - \mu \sum_i n_i, \tag{4}$$

where n_i is the usual occupation variable equal to 0 (1) when the site i is empty (occupied). The first sum runs over all nearest neighbor pairs of sites, the second sum runs over all lattice sites, and μ is the chemical potential. The energies and chemical potential in our model are expressed in units of w. The temperature is measured in units of $|w|/R$, where R is the universal gas constant.

In this paper, we have studied several special cases of the proposed model on a triangular lattice with coordination number $n_c = 6$. The special cases differ in the symmetry (c) and number of rotational states (n) of the adsorbed molecule.

(i) $c = 1$ and $n = 6, 12$. These models correspond to the adsorption layer of molecules with a C_1 symmetry of the functional group arrangement. The adsorption layer of benzoic acid is an example.

(ii) $c = 2$ and $n = 3, 6$. In the first approximation, these models describe the orientational ordering in an adsorption layer of molecules with C_2 symmetry, for example, terephthalic acid, on a homogeneous solid surface.

(iii) $c = 3$ and $n = 2, 4, 8$. At these parameters, the model describes the ordering of adsorbed molecules with C_3 symmetry of the functional group arrangement. The well-known example of such system is a trimesic acid layer on the surface of metallic single crystals or graphite.

The number of rotational states in the proposed models is related to the lattice geometry. The smallest number of rotational states of the adsorbed molecule with symmetry c is $n_{\min} = n_c/c$. In the models with a minimum number of rotational states, the functional groups of the adsorbed molecule are codirectional with one of the lattice vectors in each state. Here, we study the models with a minimum and twice the minimum number of rotational states. In view of the increased symmetry in the $c = 3$ models, we have additionally considered the case where the number of rotational states is 4 times greater than the minimum.

The Δ parameter for all the models was varied from 0 to 1. The set of Δ values for each model was determined by the energies ε_{kl} of directed attractive interactions in the key pair

configurations (α_i, α_j). An increase of the Δ value gradually weakens the attractive interactions, eventually making some of them repulsive. For example, in the models with $c = 1$ all the interaction energies U_{ij} are either zero or attractive at $\Delta = 0$. At $\Delta = 1$ all the interaction energies U_{ij} are repulsive, except for the configuration in which both angles α_i and α_j are zero (functional groups point exactly at each other).

III. METHODS

The lattice models described above were studied by the tensor renormalization group (TRG) method. The transformation of the lattice model into a tensor network consisting of N tensors T was carried out as described in [31]. Further, the tensor network was renormalized according to the standard algorithm proposed by Levin and Nave [52]. At each step of the algorithm, the procedure of singular value decomposition of tensors is performed, leaving only χ of the largest singular values. In other words, only the most probable configurations of the system are carried over to the next algorithm step. The resulting tensors were contracted in the appropriate way. The obtained tensor network formally describes a system twice as large. The trace of this tensor network $t\text{Tr}(\otimes_{i=1}^{N} T) = \sum_i e^{\beta \mathcal{H}_i} = Z$ is the partition function of the system. Here, the letter "t" indicates the multidimensionality of the mathematical operator. The value of the partition function is obtained by contracting over all matching indices. This process should repeat until the convergence on the partition function has been reached. Thus, the resulting value of the partition function corresponds to an infinite system. In this work, χ was varied from 48 to 150 singular values depending on the convergence of the calculations. Knowing the partition function, we calculated the following thermodynamic characteristics of the model adsorption layer:

$$\frac{\Omega}{RT} = -\ln(Z), \quad \theta = -\left(\frac{\partial \Omega}{\partial \mu}\right)_T, \quad S = -\left(\frac{\partial \Omega}{\partial T}\right)_\mu, \tag{3}$$

$$\frac{H}{RT} = \frac{\Omega}{RT} + \frac{S}{R}, \quad \frac{U}{RT} = \frac{H}{RT} + \theta \frac{\mu}{RT}, \tag{4}$$

where Ω is the grand thermodynamic potential, T is the thermodynamic temperature, R is the universal gas constant, and θ is the surface coverage. H, U, and S are the total energy, potential energy, and entropy of the model adsorption layer, respectively. In principle the TRG allows one to calculate any thermodynamic characteristics of a formally infinite system. This is the main advantage of the TRG method. The disadvantage of the TRG application to the adsorption systems is the difficulty in determining the calculation error.

To verify the obtained data, we used the standard grand canonical Monte Carlo (GCMC) method as implemented in the SUSMOST software package [53]. The simulation was carried out on a triangular lattice with a linear size of $L = 60$ with periodic boundary conditions. The GCMC pseudodynamics of the model adsorption layer considers the following physical processes: adsorption, desorption, rotation, and diffusion of the adsorbed molecules. These elementary events provide a change in the state of one or a pair of lattice sites. As a result of the adsorption event, a randomly selected empty site is occupied with a molecule having one of n
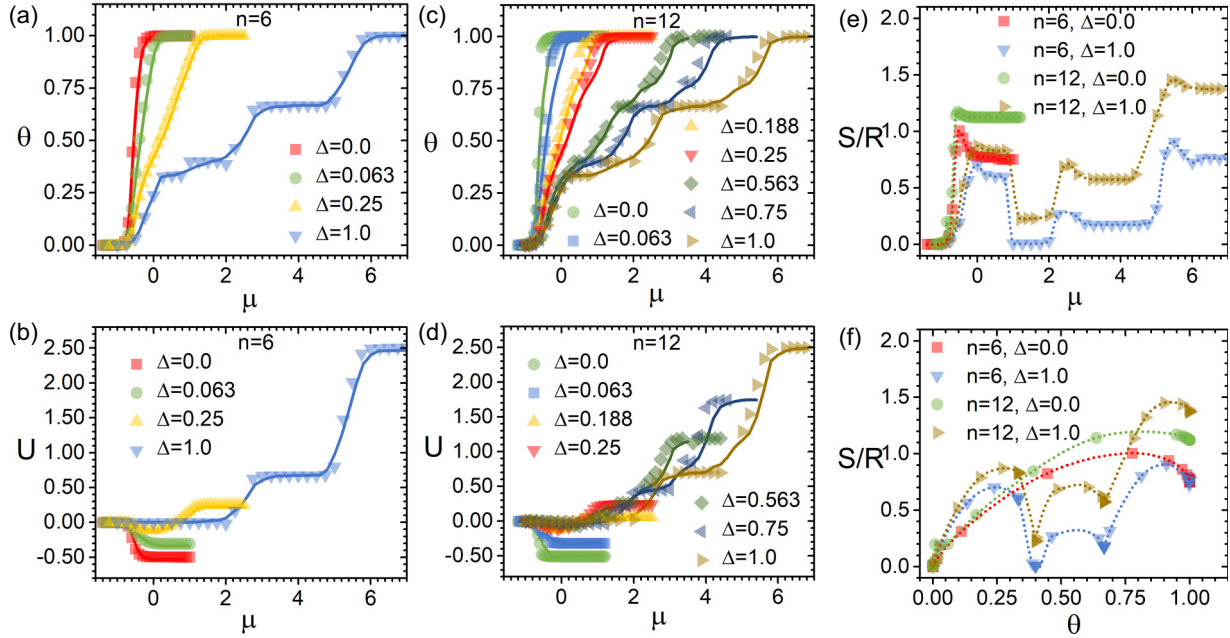
FIG. 2. Thermodynamic characteristics of the model adsorption layer of molecules with C_1 symmetry ($c = 1$) calculated for $n = 6, 12$ at the temperature $RT/|w| = 0.1$ and indicated values of the Δ parameter: (a) adsorption isotherms at $n = 6$; (b) dependences of the potential energy of the adsorption layer per lattice site on the chemical potential at $n = 6$; (c) adsorption isotherms at $n = 12$; (d) dependences of the potential energy of the adsorption layer per lattice site on the chemical potential at $n = 12$. (e), (f) show the entropy of the adsorption layer versus chemical potential (e) and coverage (f) calculated at $\Delta = 0$ and $\Delta = 1$ for both models ($n = 6, 12$). The symbols represent the results of TRG calculations, the solid line shows the GCMC results, and the dotted line is just a guide for the eyes.

possible orientations also chosen randomly. The desorption is an event opposite to the adsorption, when one of the occupied lattice sites is vacated. The rotation is a random change in the rotational state of one of the adsorbed molecules. The elementary act of diffusion was modeled as follows. A lattice site and its neighbor in the first, second, or third coordination spheres are randomly selected. Next, the states of the selected sites are exchanged. One Monte Carlo step represents $L \times L$ attempts to change the state of the model layer in one of the specified ways. To equilibrate the model adsorption layer and calculate the ensemble averages of the surface coverage and potential energy, we used 10^6 Monte Carlo steps. To improve the convergence to equilibrium state and overcome the slowing down effects the parallel tempering technique was used. The probabilities of elementary events as well as temperature switching in the system were determined by the standard Metropolis algorithm [54]. There is good agreement between the coverage and energy values of the layer obtained by the Monte Carlo and TRG methods independently. This indicates the sufficiency of the chosen lattice size and number of Monte Carlo steps.

IV. RESULTS AND DISCUSSION

This section presents the results of studying some cases of the proposed model by the TRG method at a constant temperature $RT/|w| = 0.1$. The calculation results were verified by the standard GCMC method. The considered special cases of the model relate to the well-known adsorption layers of benzoic ($c = 1$), terephthalic ($c = 2$), and trimesic ($c = 3$)

acids on a homogeneous surface of graphite or metallic single crystals.

A. Adsorption of the molecules with C_1 symmetry

Figures 2(a) and 2(c) show the dependences of surface coverage on the chemical potential (hereinafter called *adsorption isotherms*) calculated for the molecules with C_1 symmetry at $n = 6$ and $n = 12$ and different values of the Δ parameter. Recall that Δ describes in the first approximation the effective isotropic repulsions between molecules adsorbed at neighboring lattice sites. The corresponding dependences of the potential energy of the adlayer per lattice site on the chemical potential are illustrated in Figs. 2(b) and 2(d). An increase in the number of rotational states n in this model has practically no effect on the shape of the adsorption isotherms and potential energy curves. Depending on the Δ value, one can distinguish from one to four horizontal plateaus on the adsorption isotherms and $U(\mu)$ curves. These plateaus correspond to stable phases of the molecular layer. Note that the results obtained by fundamentally different methods are in good agreement. The deviations between the TRG and Monte Carlo curves do not exceed the symbol size in most cases. An exception is the μ range near the phase transition to a dense phase ($\theta = 1$) in the model with $c = 1$, $n = 12$. The error of Monte Carlo calculations is known to increase significantly in the phase transition region due to an increase of the autocorrelation time [54].

If the directed attractive interactions clearly prevail over the isotropic repulsions ($\Delta \ll 1$), then an abrupt change from zero to full surface coverage occurs when chemical potential
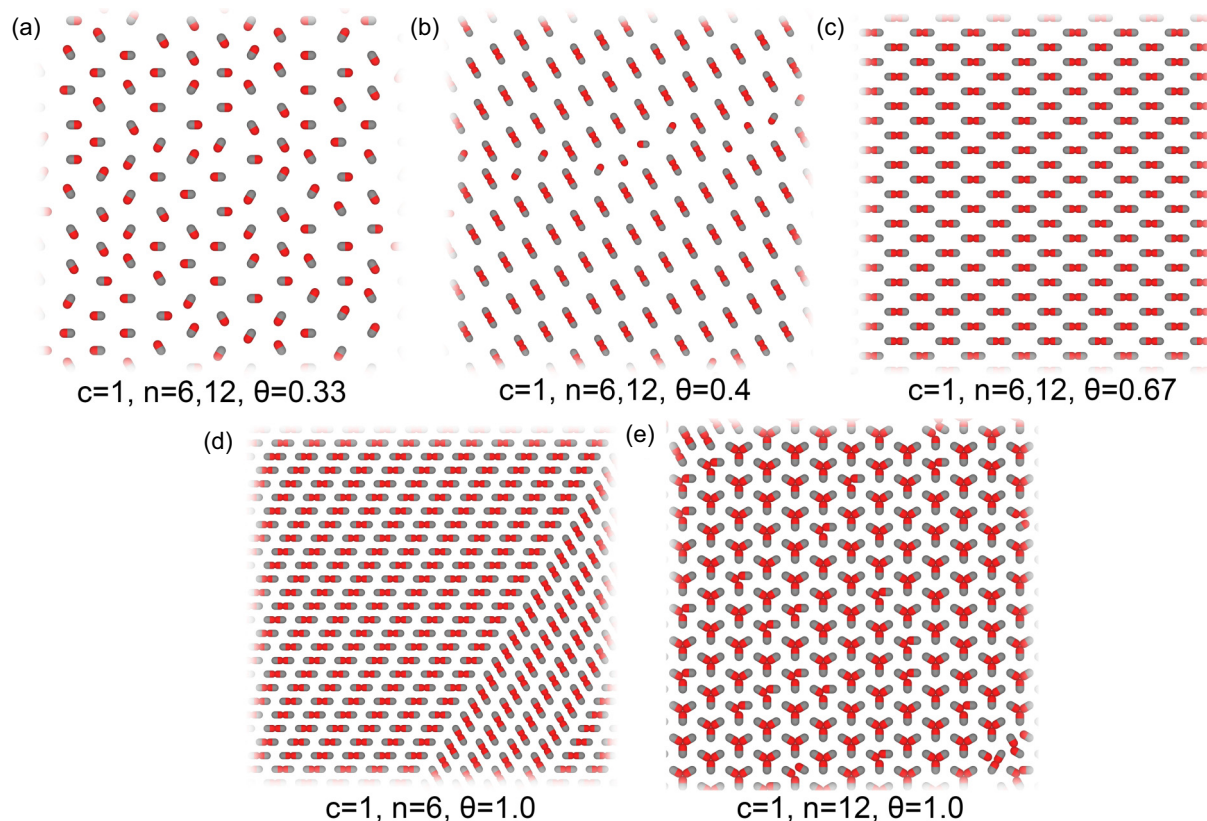
FIG. 3. Snapshots of the equilibrated adlayer of the molecules with C_1 symmetry ($c = 1$) made during the GCMC simulation at $RT/|w| = 0.1$ and different values of the chemical potential. The number of rotational states used in the model and surface coverage related to each adlayer structure are indicated below the snapshots. To make the snapshots clearer we show only a part of the lattice.

increases. At higher values of the Δ parameter, the transition from the surface gas ($\theta \approx 0$) to a dense structure ($\theta = 1$) smooths out and shifts towards higher values of the chemical potential. A further increase of Δ induces the self-assembly of three extra phases at $\theta \approx 0.33$, $\theta \approx 0.4$, and $\theta \approx 0.66$. At $\Delta \geqslant 0.75$, there are four stable phases of different densities in the adlayer. The corresponding dependences of the potential energy on the chemical potential also indicate the appearance of these stable phases. Thus, the porous phases ($\theta < 1$) in such systems appear only in the presence of competing attractive and repulsive interactions. As can be seen, the sequential formation of the porous phases is characterized by the monotonic and everywhere positive $U(\mu)$ dependences. Potential energies of these phases can be estimated from the position of horizontal plateaus in the $U(\mu)$ curves [Figs. 2(b) and 2(d)]. The potential energies of the model adsorption layer per lattice site in the phases with $\theta \approx 0.33$ and $\theta \approx 0.4$ are equal to zero at $\Delta = 1$. In these phases, the molecules either do not interact, or the attraction and repulsion interactions compensate each other. In the phase with $\theta \approx 0.66$, the potential energy of the layer per lattice site is close to 0.67 (or 1.0 per molecule). The potential energies of the dense phases in both models are close to 2.5.

Figure 2(e) demonstrates the changing of the layer entropy versus the chemical potential in two limit cases of the interactions in the adlayer: (i) no repulsive interactions ($\Delta = 0$); (ii) no attractive interactions ($\Delta = 1$). On the $S(\mu)$ curves for both models one can see either one plateau at $\Delta = 0$

or four plateaus at $\Delta = 1$. These plateaus correspond to the stable phases described above. Positions of the minima in the dependences of the entropy on the surface coverage at $\Delta = 1$ [Fig. 2(f)] reveal that porous structures are ordered. An exception is the phase with $\theta \approx 0.33$. There is no pronounced minimum of the entropy at this surface coverage. There is only a clustering of points. Thus, the stable phase at $\theta \approx 0.33$ is disordered.

To identify the structure of the stable phases, we took snapshots of the model adsorption layer during the Monte Carlo simulation (Fig. 3). The phase with coverage $\theta \approx 0.33$ is indeed orientationally disordered [Fig. 3(a)]. In this phase, the nearest neighborhood of adsorbed molecules is excluded. Therefore, the potential energy of this phase is equal to zero. An increase of the chemical potential leads to dimerization of single molecules due to the directed interaction between their functional groups. In the resulting phase ($\theta \approx 0.4$), a nearest neighborhood of the dimers, rather than individual molecules, is excluded [Fig. 3(b)]. The potential energy of this phase is also zero at $\Delta = 1$. At $\Delta = 1$, only the direct interaction between the functional groups ($\alpha_i = 0$, $\alpha_j = 0$) is equal to zero. The interaction energy in other mutual orientations of the neighboring molecules is repulsive (positive). A further increase in the chemical potential favors a compaction of the dimer packing. Initially, a phase where each dimer is adjacent to four other dimers ($\theta \approx 0.66$) appears [Fig. 3(c)]. Therefore, the potential energy of this phase is positive. The structure of the dense phase depends on the number of rotational states
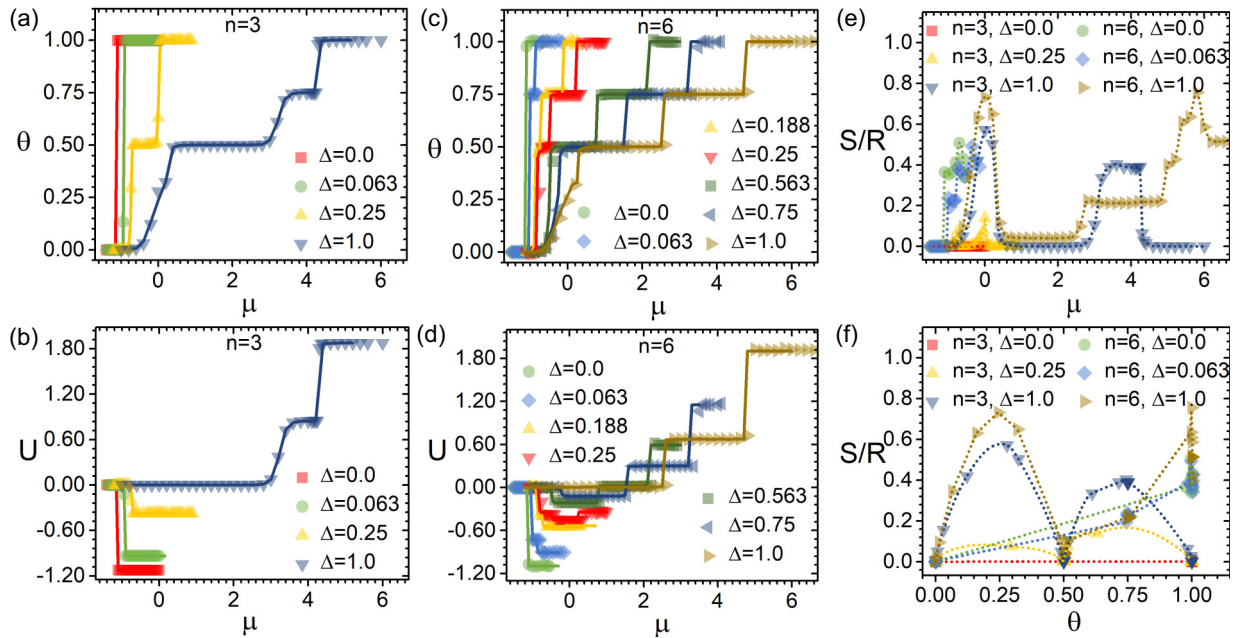
FIG. 4. Thermodynamic characteristics of the model adsorption layer of molecules with C_2 symmetry ($c = 2$) calculated for $n = 3, 6$ at the temperature $RT/|w| = 0.1$ and indicated values of Δ parameter: (a), (c) the adsorption isotherms for $n = 3$ and $n = 6$, respectively; (b), (d) the potential energy of the adsorption layer per lattice site versus the chemical potential calculated for $n = 3$ and $n = 6$, respectively; (e), (f) show the dependences of molecular layer entropy on the chemical potential and surface coverage calculated at $\Delta = 0, 0.063, 0.25, 1.0$ for both models ($n = 3$ and $n = 6$). The symbols represent the results of TRG calculations, the solid line shows the GCMC results, and the dotted line is just a guide for the eyes.

considered in the model. At $n = 6$, the dense phase consists of parallel chains of the dimers [Fig. 3(d)]. In the case of $n = 12$, the dense phase represents a mixture of close packed tripod [Fig. 3(e)] and linear [Fig. 3(d)] structures. According to the results of TRG and GCMC simulations the potential energies of these structures at $\Delta = 1.0$ differ only by 0.01. However, the entropy of the dense phase at $n = 12$ considerably depends on Δ and always exceed the entropy of the dense linear structure appearing at $n = 6$ [Figs. 2(e) and 2(f)]. Therefore, the existence of a stable mixture of linear and tripod close packed structures in the model adlayer at $n = 12$ seems to be entropy driven.

Thus, the phase behavior of the adsorption layer of monofunctional molecules has a hierarchical character. Firstly, due to strong attractive interactions dimerization of the monofunctional molecules occurs. Further increasing the surface coverage induces the self-assembly of the dimers into more complex structures due to weak interactions. Similar phase behavior is experimentally observed in the adsorption layer of benzoic acid on the Au(111) surface [55,56]. In addition, the STM images reveal the formation of ring-based bonding motifs [56] like trimers in the herringbone structure.

B. Adsorption of the molecules with C_2 symmetry

This section presents the results of modeling the self-assembly of bifunctional molecules with C_2 symmetry. In this case, we consider two models that differ in the number of rotational states of the adsorbed molecule. The calculated dependences of the surface coverage, potential energy, and entropy of the layer on the chemical potential are shown in

Fig. 4. As seen, the results obtained by the TRG coincide with the results of standard Monte Carlo simulation. This confirms the correctness of the implemented TRG algorithm. All calculated curves demonstrate that an increase of the isotropic repulsions (Δ) between neighboring molecules leads to a diverse phase behavior of the model adsorption layer.

In the absence of repulsive interactions (Δ close to zero), the adsorption isotherms [Figs. 4(a) and 4(c)] and the dependences of potential energy of the adlayer on the chemical potential [Figs. 4(b) and 4(d)] show a single plateau corresponding to a stable dense phase. At small values of the Δ parameter, one additional plateau appears on the $\theta(\mu)$ and $U(\mu)$ curves: at $\theta = 0.5$ for the $c = 2$, $n = 3$ model and $\theta = 0.75$ for the $c = 2$, $n = 6$ model. At relatively large Δ, there are three plateaus on the adsorption isotherms at $\theta = 0.5$, $\theta = 0.75$, and $\theta = 1.0$. When $\Delta = 1.0$, the $\Delta\mu$ regions of existence of a stable phase with $\theta = 0.75$ and entropy of the molecular layer at this coverage differ significantly in the models $n = 3$ and $n = 6$. The entropies of dense phases in these models are also different [Figs. 4(e) and 4(f)]. These observations allow us to conclude that structures of stable phases at $\theta = 0.75$ and $\theta = 1.0$ depend on the number of rotational states of the adsorbed molecule used in the model.

Figure 5 illustrates the structures of stable phases obtained in the GCMC simulations at $c = 2$, $n = 3$ and $c = 2$, $n = 6$. The phase with $\theta = 0.5$ has the same structure in both models and consists of linear chains [Fig. 5(a)]. The molecules composing the chains are linked by hydrogen bonds. Parallel molecular chains in this structure do not interact with each other, because of the long distance between them. Recall that in this model we consider only nearest neighbor
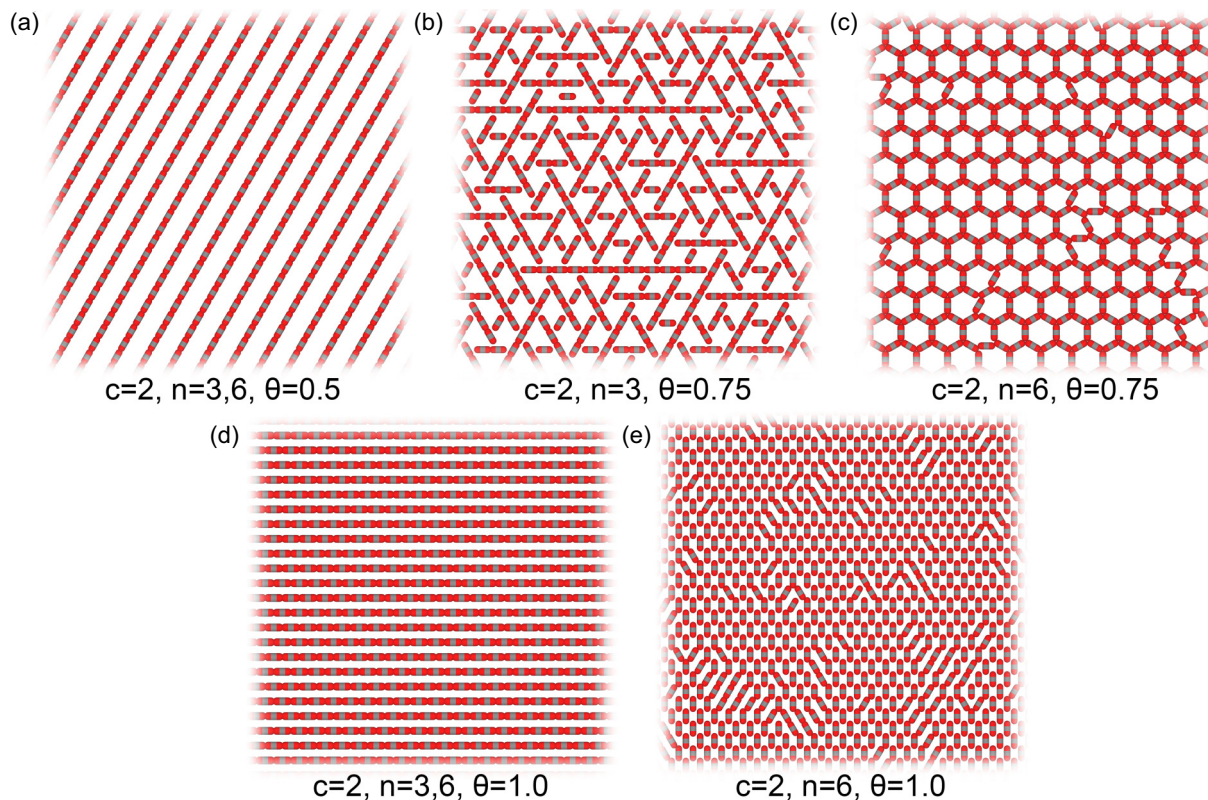
FIG. 5. Snapshots of the equilibrated adlayer in the $c = 2$, $n = 3$ and $c = 2$, $n = 6$ models obtained during the GCMC simulation at the temperature $RT/|w| = 0.1$. The number of rotational states used in the model and surface coverage related to each adlayer structure are indicated below the snapshots. To make the snapshots clearer we show only a part of the lattice.

interactions. As we suggested above, the structure of the phase with coverage $\theta = 0.75$ is indeed different in the $n = 3$ and $n = 6$ models. Due to the larger number of rotational states in the $c = 2$, $n = 6$ model a honeycomb structure is formed [Fig. 5(c)]. At the same value of the chemical potential, a ladder phase appears in the model $c = 2$, $n = 3$ [Fig. 5(b)]. The potential energy of the honeycomb structure (0.67 per lattice site) is significantly lower than the potential energy of the ladder structure (≈ 0.85 per lattice site). Apparently, this compensates for the lower entropy of the honeycomb structure compared to the ladder one [Fig. 5(f)]. A more subtle effect explains the difference between the entropies of the dense structures appearing in the $n = 3$ and $n = 6$ models. In the $c = 2$, $n = 6$ model, the dense phase is a superposition of two energetically equivalent structures: linear [Fig. 5(d)] and "brick wall" [Fig. 5(e)]. During the GCMC simulation, these structures are always switched. Due to the smaller number of rotational states in the $c = 2$, $n = 3$ model the brick structure cannot be formed.

Linear structures of different density [Figs. 5(a) and 5(d)] and the brick-wall structure [Fig. 5(e)] are observed experimentally in adsorption layers of terephthalic acid on the surface of metallic single crystals and graphite [11,57–64]. As far as we know, the ladder and honeycomb structures still not been observed in the STM experiments. This indicates the absence of significant repulsive interactions in the adsorption layer of terephthalic acid or/and the insufficient accuracy of the experimental techniques.

C. Adsorption of the molecules with C_3 symmetry

We have studied three lattice models of the adsorption layer comprising the trifunctional molecules with C_3 symmetry of the arrangement of functional groups ($c = 3$). The models differ only in the number of rotational states of the adsorbed molecule: $n = 2$, 4, and 8. In Figs. 6(a) and 6(b) the dependences of surface coverage and potential energy of the molecular layer on the chemical potential are shown. We demonstrate the calculated thermodynamic characteristics only for the $c = 3$, $n = 2$ model, because they are practically independent of n. The effect of the number of rotational states in the $c = 3$ model can be estimated in Figs. 6(c) and 6(d). An increase in the number of rotational states of the adsorbed molecule leads to rounding and shifting of phase transitions towards lower μ values. As in the previous cases, the results obtained by the TRG and GCMC methods are in excellent agreement. However, the adsorption isotherms and potential energy curves calculated by the TRG method are smoothed in comparison with the corresponding curves obtained by the GCMC method.

In the absence of isotropic repulsions between the nearest neighbor molecules ($\Delta = 0$) a gradual growth of the chemical potential causes spontaneous condensation of the surface gas into a dense phase ($\theta = 1.0$). When Δ increases from 0 to 1, a horizontal plateau on the adsorption isotherms at $\theta \approx 0.67$ appears and expands in the μ region between the lattice gas ($\theta = 0$) and dense phase ($\theta = 1.0$). The extra plateau also appears on the $U(\mu)$ curves. This indicates the formation of
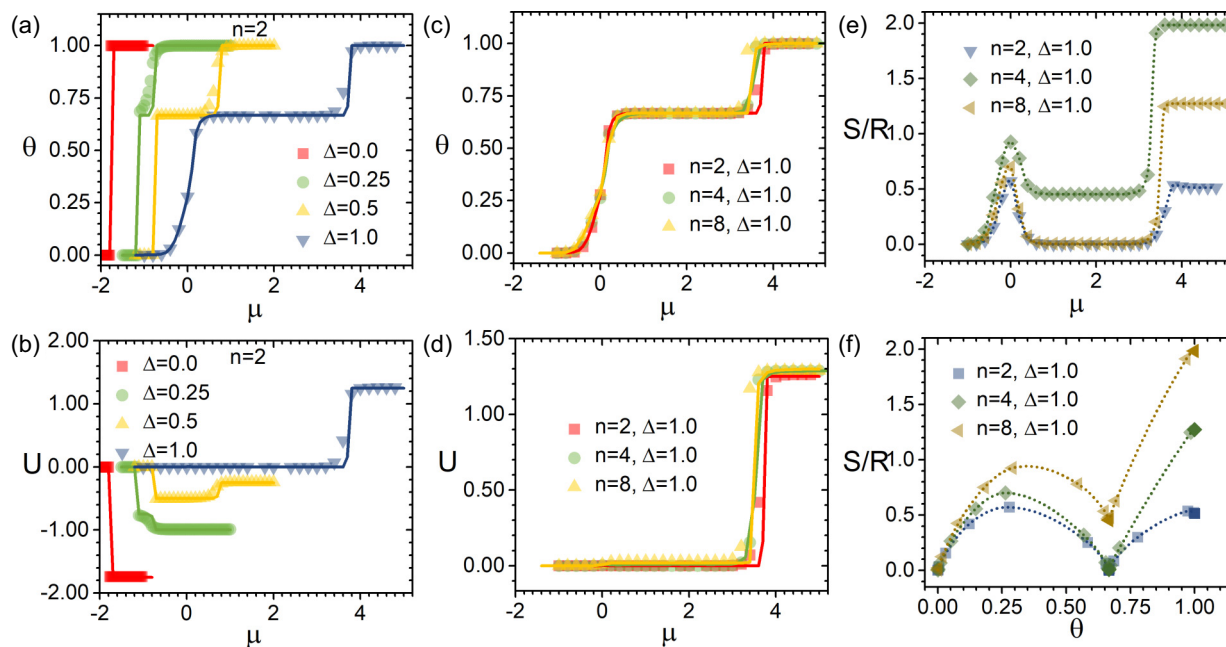
FIG. 6. Thermodynamic characteristics of the model adsorption layer of trifunctional molecules with C_3 symmetry ($c = 3$) calculated for $n = 2, 4, 8$ at the temperature $RT/|w| = 0.1$ and indicated values of the Δ parameter: (a) adsorption isotherms and (b) dependences of the layer potential energy on the chemical potential in the model $c = 3$, $n = 2$; (c) adsorption isotherms and (d) dependences of the layer potential energy on the chemical potential calculated at $\Delta = 1.0$ in models with different numbers of rotational states $n = 2, 4, 8$. (e), (f) show the dependences of adsorption layer entropy on the chemical potential (e) and surface coverage (f) calculated at $\Delta = 1.0$ and $n = 2, 4, 8$. The symbols represent the results of TRG calculations, the solid line shows the GCMC results, and the dotted line is just a guide for the eyes.

a stable porous structure in the adsorption layer. The μ region of existence of this structure is practically independent of n.

Figures 6(e) and 6(f) illustrate the change of entropy of the $c = 3$ molecular layer with surface coverage and chemical potential. Horizontal plateaus on the $S(\mu)$ curves and minima on the $S(\theta)$ curves confirm the sequential self-assembly of two stable phases in the molecular layer at $\theta \approx 0.67$ and $\theta = 1.0$. Moreover, the entropy of the porous structure at $\theta \approx 0.67$ is less than the entropy of the dense phase.

Visualization of the model adsorption layers (Fig. 7) obtained during the Monte Carlo simulation allowed us to

identify the phase structure at $\theta \approx 0.67$ and $\theta = 1.0$. The snapshots of the model adsorption layer were also used to find out the reason for the significant difference in the entropy values of the dense phase in the $c = 3$ models with different numbers of rotational states $n = 2, 4, 8$.

It is seen in Fig. 7(a) that the surface gas at nonzero Δ condensates into the honeycomb structure with surface coverage $\theta \approx 0.67$. This phase is typical for the $c = 3$ models with any number of rotational states. Self-assembly of the honeycomb structure is observed experimentally in the adsorption layers of trimesic acid on the surface of metallic single crystals
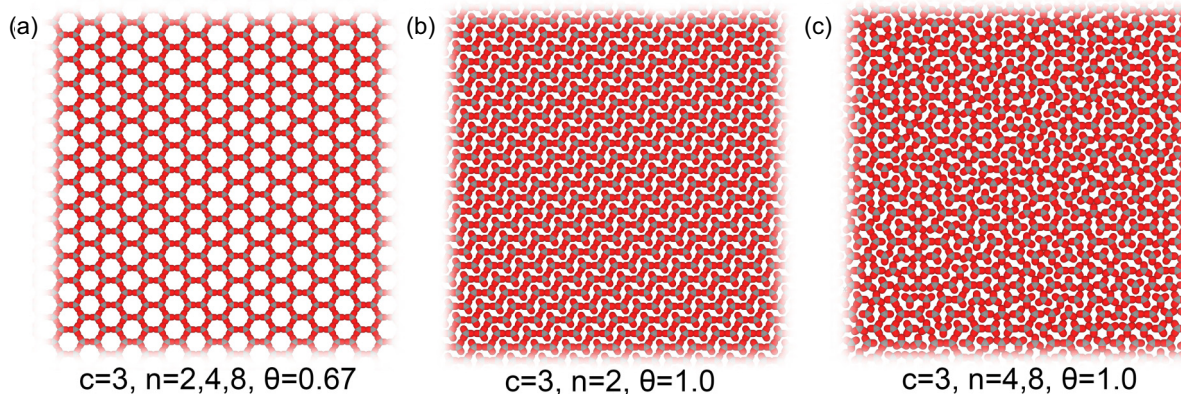

c=3, n=2,4,8, θ=0.67   c=3, n=2, θ=1.0   c=3, n=4,8, θ=1.0

FIG. 7. Snapshots of the equilibrated adsorption layer of the molecules with C_3 symmetry ($c = 3$) and different number of rotational states $n = 2, 4, 6$ made during the GCMC simulation at $RT/|w| = 0.1$ and different values of the chemical potential. The number of rotational states used in the model and surface coverage related to each adlayer structure are indicated below the snapshots. To make the snapshots clearer we show only a part of the lattice.
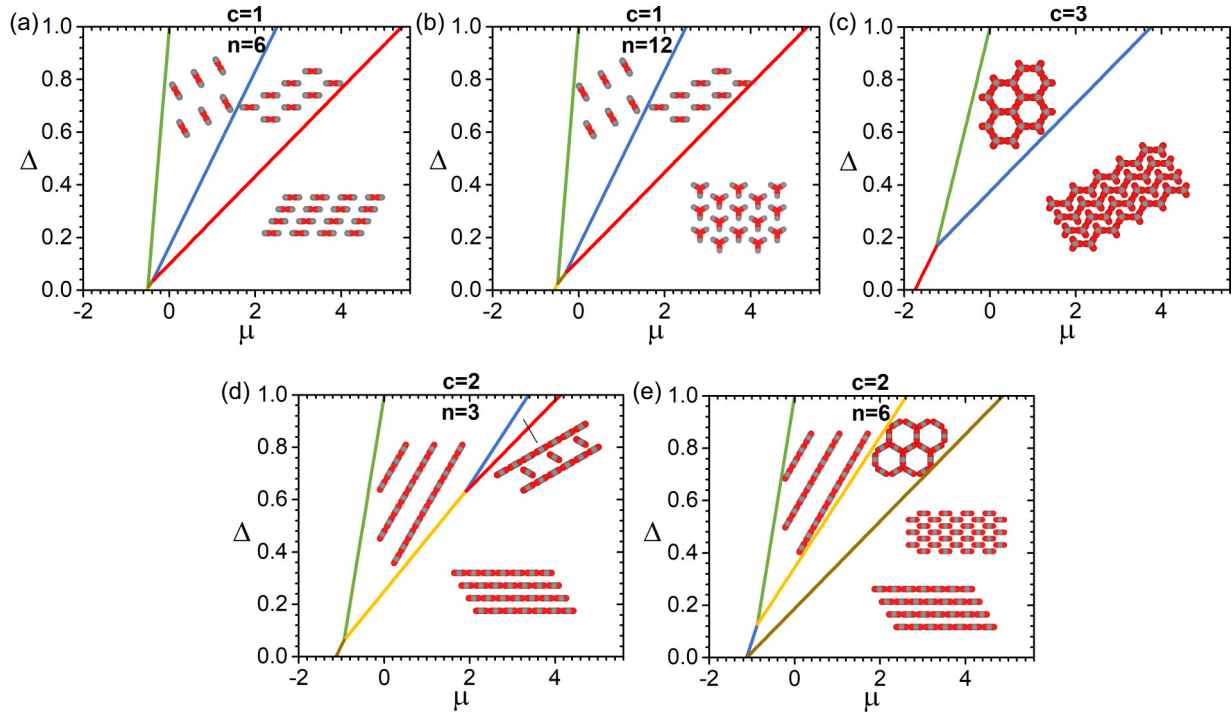
FIG. 8. Ground state phase diagrams of the model adsorption layers of molecules with C_1, C_2, C_3 symmetry of the functional group arrangement.

[65–67] and graphite [68,69]. The dense phase in the $c = 3$, $n = 2$ model has an ordered zigzag structure. In the $c = 3$, $n = 4$ and $c = 3$, $n = 8$ models, the dense phase is disordered and represents a mixture of three structural elements: zigzags, filled honeycombs, and triangular trimers of identically oriented molecules. Elements of the zigzag structure are observed on the STM images of the trimesic acid adsorption layer on the copper surface [67,70].

D. Ground state of the models and entropic effects

Our TRG calculations and Monte Carlo simulations allow us to establish a set of stable and metastable self-assembling structures in the model adsorption layers of molecules with C_1, C_2, C_3 symmetry at the constant temperature of $RT/|w| = 0.1$. Knowing the structure of these phases, one can analyze the ground state of the models. Indeed, the grand thermodynamic potential of the adsorption layer at $RT/|w| = 0$ depends only on the chemical potential and energies of the intermolecular interactions. An entropy contribution to the free energy at $RT/|w| = 0$ is zero. Using the principle of the minimum of the grand thermodynamic potential, we have determined the (μ, Δ) regions of existence for each structure in the ground state of the model. The obtained ground state phase diagrams of the model adsorption layers in (μ, Δ) coordinates are shown in Fig. 8. It is seen that structures of the phase diagrams at $c = 1$ and $c = 2$ depend on the number of rotational states of the adsorbed molecule. In the $c = 1$ model the phase coexistence lines calculated at $n = 6$ and $n = 12$ coincide, but the structures of the dense phases differ. The phase diagrams for the $c = 2$ model calculated at $n = 3$ and $n = 6$ are completely different. In the case of $c = 3$, changing

the number of rotational states does not affect the structure of the phase diagram.

In the ground state of the $c = 1$ model the orientationally disordered phase [Fig. 3(a)], where the nearest neighborhood of adsorbed molecules is excluded, does not appear. The potential energy of this orientationally disordered phase is equal to zero. Therefore, its self-assembly at nonzero temperatures is driven only by the chemical potential and entropy of the molecular layer. Structures of the dense phases in the $c = 1$, $n = 12$ model at zero and nonzero temperatures are different. In the ground state of the model the tripod close packed phase appears, but at nonzero temperatures, the dense phase in the $c = 1$, $n = 12$ model represents a mixture of close packed tripod [Fig. 3(e)] and linear [Fig. 3(d)] structures. The tripod and linear structures have the same density $\theta = 1.0$, and their potential energies at $\Delta = 1.0$ differ by 0.03. This points to the entropic nature of the self-assembly of the dense phase in the $c = 1$, $n = 12$ model.

The phase behavior of the $c = 2$ models at nonzero temperature fully corresponds to the ground state of these models, including the superposition of dense phase structures at $n = 6$. The latter indicates that density, potential energy, and entropy of the linear and brick-wall phases in the studied range of the model parameters are equal.

According to our TRG and GCMC simulations, the dense phase in the $c = 3$, $n = 4$ and $c = 3$, $n = 8$ models at nonzero temperatures is disordered and represents a mixture of different structures. Among them, one can distinguish zigzags, filled honeycombs, and triangular trimers of identically oriented molecules. The potential energy of this disordered structure obtained by the TRG and Monte Carlo methods at $\Delta = 1.0$ is equal to $U \approx 1.29$. This is an intermediate value

between the energies of zigzag (1.25), filled honeycomb (1.25), and "triangular" (1.31) structures. Despite the relatively high potential energy of the triangular phase, its elements are observed in the model adsorption layers. It can be explained by the configurational entropy of the structures. The unit cell of the triangular phase (1×1) is smaller than the unit cells of the zigzag (1×2) and filled honeycomb (3×3) structures. From this point of view, the self-assembly of the triangular phase is favorable.

V. CONCLUSION

In this work, we have demonstrated the successful application of the tensor renormalization group (TRG) for the analysis of orientational ordering in organic adsorption layers with directed intermolecular interactions. Additionally, we have developed a simple lattice model of the adsorption layer, which takes into account the rotational symmetry of the adsorbed molecule as well as the directionality of intermolecular interactions. Phase behaviors of several special cases of the proposed general model have been studied at the constant temperature $RT/|w| = 0.1$ by the TRG and Monte Carlo methods in the grand canonical ensemble. All the considered models differ in the symmetry and number of rotational states of the adsorbed molecule. The prototype systems for the models studied in this work are the well-known adsorption layers of benzoic, terephthalic, and trimesic acids on homogeneous surfaces of metallic single crystals and the highly ordered pyrolytic graphite.

Summarizing the results of our simulations, we can draw the following conclusions:

(i) The TRG can be successfully used to analyze the orientational ordering in molecular layers on solid surfaces. The thermodynamic characteristics of the model adsorption layer calculated by the TRG method are reproduced by the standard Monte Carlo simulation. However, the TRG has several important advantages. This approach is free from finite size effects and allows one to directly calculate the partition function of the lattice model. Thus, using the TRG method it is possible to compute any thermodynamic characteristics for a formally infinite system. For example, in this work, we have calculated the entropy of the model adsorption layers. Solving this problem by the Monte Carlo method is much more laborious.

(ii) Our model qualitatively reproduces the phase behavior of the real adsorption layers of benzoic, terephthalic, and trimesic acids on homogeneous solid surfaces. Therefore, the proposed model can be used to interpret experimental data as well as to predict the phase behavior of an organic adsorption layer from the chemical structure of the adsorbate molecule and adsorbent surface. For example, our model of the adsorption layer of bifunctional (bicarboxyl) molecules with C_2 symmetry predicts the self-assembly of honeycomb and/or ladder phases.

(iii) An essential role in the self-assembly of dense phases in organic adsorption layers is played by entropy effects. Therefore, the number of rotational states included in the model affects the structure of dense phases.

An independent application of the TRG to study complex adsorption systems requires an algorithm for visualizing a model adsorption layer or some analog of the order parameter determined directly from the tensor structure at each iteration of the TRG algorithm. These are the subjects of our future research.

[1] J. V. Barth, G. Costantini, and K. Kern, Engineering atomic and molecular nanostructures at surfaces, Nature (London) **437**, 671 (2005).

[2] J. V. Barth, Molecular architectonic on metal surfaces, Annu. Rev. Phys. Chem. **58**, 375 (2007).

[3] J. MacLeod, Design and construction of on-surface molecular nanoarchitectures: Lessons and trends from trimesic acid and other small carboxylated building blocks, J. Phys. D: Appl. Phys. **53**, 043002 (2019).

[4] K. S. Mali, N. Pearce, S. De Feyter, and N. R. Champness, Frontiers of supramolecular chemistry at solid surfaces, Chem. Soc. Rev. **46**, 2520 (2017).

[5] D. B. Amabilino and S. L. Tait, Complex molecular surfaces and interfaces: Concluding remarks, Faraday Discuss. **204**, 487 (2017).

[6] A. Ciesielski, P. J. Szabelski, W. Rżysko, A. Cadeddu, T. R. Cook, P. J. Stang, and P. Samorì, Concentration-dependent supramolecular engineering of hydrogen-bonded nanostructures at surfaces: Predicting self-assembly in 2D, J. Am. Chem. Soc. **135**, 6942 (2013).

[7] D. Ecija, M. Marschall, J. Reichert, A. Kasperski, D. Nieckarz, P. Szabelski, W. Auwärter, and J. V. Barth, Dynamics and thermal stability of surface-confined metal–organic chains, Surf. Sci. **643**, 91 (2016).

[8] A. Kasperski and P. Szabelski, Two-dimensional molecular sieves: Structure design by computer simulations, Adsorption **19**, 283 (2012).

[9] S. Whitelam and I. Tamblyn, Learning to grow: Control of material self-assembly using evolutionary reinforcement learning, Phys. Rev. E **101**, 052604 (2020).

[10] P. Kocán, B. Pieczyrak, L. Jurczyszyn, Y. Yoshimoto, K. Yagyu, H. Tochihara, and T. Suzuki, Self-ordering of chemisorbed PTCDA molecules on Ge(001) driven by repulsive forces, Phys. Chem. Chem. Phys. **21**, 9504 (2019).

[11] T. W. White, N. Martsinovich, A. Troisi, and G. Costantini, Quantifying the "subtle interplay" between intermolecular and molecule–substrate interactions in molecular assembly on surfaces, J. Phys. Chem. C **122**, 17954 (2018).

[12] A. Ibenskas, M. Šimėnas, and E. E. Tornau, Numerical engineering of molecular self-assemblies in a binary system of trimesic and benzenetribenzoic acids, J. Phys. Chem. C **120**, 6669 (2016).

[13] A. Rastgoo-Lahrood, N. Martsinovich, M. Lischka, J. Eichhorn, P. Szabelski, D. Nieckarz, T. Strunskus, K. Das, M. Schmittel,

W. M. Heckl *et al.*, From Au–thiolate chains to thioether Sierpiński triangles: The versatile surface chemistry of 1,3,5-tris(4-mercaptophenyl) benzene on Au(111), ACS Nano **10**, 10901 (2016).

[14] M. El Garah, A. Dianat, A. Cadeddu, R. Gutierrez, M. Cecchini, T. R. Cook, A. Ciesielski, P. J. Stang, G. Cuniberti, and P. Samorì, Atomically precise prediction of 2D self-assembly of weakly bonded nanostructures: STM insight into concentration-dependent architectures, Small **12**, 343 (2016).

[15] M. Mura and F. Silly, Experimental and theoretical analysis of hydrogen bonding in two-dimensional chiral $4', 4''''$-$(1, 4-phenylene)bis(2, 2' : 6', 2''-terpyridine)$ self-assembled nanoarchitecture, J. Phys. Chem. C **119**, 27125 (2015).

[16] A. I. Livshits and L. Kantorovich, Guanine assemblies on the Au(111) surface: A theoretical study, J. Phys. Chem. C **117**, 5684 (2013).

[17] S. Conti and M. Cecchini, Predicting molecular self-assembly at surfaces: A statistical thermodynamics and modeling approach, Phys. Chem. Chem. Phys. **18**, 31480 (2016).

[18] J. F. Dienstmaier, K. Mahata, H. Walch, W. M. Heckl, M. Schmittel, and M. Lackinger, On the scalability of supramolecular networks—high packing density vs optimized hydrogen bonds in tricarboxylic acid monolayers, Langmuir **26**, 10708 (2010).

[19] D. K. Jacquelín, F. A. Soria, P. A. Paredes-Olivera, and E. M. Patrito, Reactive force field-based molecular dynamics simulations on the thermal stability of trimesic acid on graphene: implications for the design of supramolecular networks, ACS Appl. Nano Mater. **4**, 9241 (2021).

[20] V. A. Gorbunov, S. S. Akimenko, A. V. Myshlyavtsev, V. F. Fefelov, and M. D. Myshlyavtseva, Adsorption of triangular-shaped molecules with directional nearest-neighbor interactions on a triangular lattice, Adsorption **19**, 571 (2013).

[21] S. S. Akimenko, V. A. Gorbunov, A. V. Myshlyavtsev, and V. F. Fefelov, Self-organization of monodentate organic molecules on a solid surface—a Monte Carlo and transfer-matrix study, Surf. Sci. **639**, 89 (2015).

[22] S. S. Akimenko, V. A. Gorbunov, A. V. Myshlyavtsev, and P. V. Stishenko, Generalized lattice-gas model for adsorption of functional organic molecules in terms of pair directional interactions, Phys. Rev. E **93**, 062804 (2016).

[23] A. Ibenskas and E. E. Tornau, Statistical model for self-assembly of trimesic acid molecules into homologous series of flower phases, Phys. Rev. E **86**, 051118 (2012).

[24] T. Misiūnas and E. E. Tornau, Ordered assemblies of triangular-shaped molecules with strongly interacting vertices: Phase diagrams for honeycomb and zigzag structures on triangular lattice, J. Phys. Chem. B **116**, 2472 (2012).

[25] A. Ibenskas, M. Šimėnas, and E. E. Tornau, Multiorientation model for planar ordering of trimesic acid molecules, J. Phys. Chem. C **122**, 7344 (2018).

[26] P. Szabelski, W. Rżysko, T. Pańczyk, E. Ghijsens, K. Tahara, Y. Tobe, and S. De Feyter, Self-assembly of molecular tripods in two dimensions: Structure and thermodynamics from computer simulations, RSC Adv. **3**, 25159 (2013).

[27] D. Nieckarz and P. Szabelski, Simulation of the self-assembly of simple molecular bricks into Sierpiński triangles, Chem. Commun. **50**, 6843 (2014).

[28] D. Nieckarz, W. Rżysko, and P. Szabelski, On-surface self-assembly of tetratopic molecular building blocks, Phys. Chem. Chem. Phys. **20**, 23363 (2018).

[29] V. A. Gorbunov, S. S. Akimenko, and A. V. Myshlyavtsev, Cross-impact of surface and interaction anisotropy in the self-assembly of organic adsorption monolayers: A Monte Carlo and transfer-matrix study, Phys. Chem. Chem. Phys. **19**, 17111 (2017).

[30] S. S. Akimenko, A. V. Myshlyavtsev, M. D. Myshlyavtseva, V. A. Gorbunov, S. O. Podgornyi, and O. S. Solovyeva, Tri-angles on a triangular lattice: Insights into self-assembly in two dimensions driven by shape complementarity, Phys. Rev. E **105**, 044104 (2022).

[31] S. S. Akimenko, V. A. Gorbunov, A. V. Myshlyavtsev, and P. V. Stishenko, Tensor renormalization group study of hard-disk models on a triangular lattice, Phys. Rev. E **100**, 022108 (2019).

[32] K. Yoshiyama and K. Hukushima, Higher-order tensor renor-malization group approach to lattice glass model, J. Phys. Soc. Jpn. **89**, 104003 (2020).

[33] A. A. A. Jaleel, D. Mandal, and R. Rajesh, Hard core lattice gas with third next-nearest neighbor exclusion on triangular lattice: One or two phase transitions? J. Chem. Phys. **155**, 224101 (2021).

[34] A. A. A. Jaleel, D. Mandal, J. E. Thomas, and R. Rajesh, Freez-ing phase transition in hard-core lattice gases on the triangular lattice with exclusion up to seventh next-nearest neighbor, Phys. Rev. E **106**, 044136 (2022).

[35] V. Berezinskii, Destruction of long-range order in one-dimensional and two-dimensional systems having a continuous symmetry group. I. Classical systems, Zh. Eksp. Teor. Fiz. **59**, 907 (1971) [Sov. Phys. JETP **32**, 493 (1971)].

[36] J. M. Kosterlitz and D. J. Thouless, Ordering, metastability and phase transitions in two-dimensional systems, J. Phys. C: Solid State Phys. **6**, 1181 (1973).

[37] J. Tobochnik, Properties of the q-state clock model for $q = 4$, 5, and 6, Phys. Rev. B **26**, 6201 (1982).

[38] P. Minnhagen, The two-dimensional Coulomb gas, vortex un-binding, and superfluid-superconducting films, Rev. Mod. Phys. **59**, 1001 (1987).

[39] J. F. Yu, Z. Y. Xie, Y. Meurice, Y. Liu, A. Denbleyker, H. Zou, M. P. Qin, J. Chen, and T. Xiang, Tensor renormalization group study of classical *XY* model on the square lattice, Phys. Rev. E **89**, 013308 (2014).

[40] J. Chen, H.-J. Liao, H.-D. Xie, X.-J. Han, R.-Z. Huang, S. Cheng, Z.-C. Wei, Z.-Y. Xie, and T. Xiang, Phase transition of the q-state clock model: Duality and tensor renormalization, Chin. Phys. Lett. **34**, 050503 (2017).

[41] Z. Q. Li, L. P. Yang, Z. Y. Xie, H. H. Tu, H. J. Liao, and T. Xiang, Critical properties of the two-dimensional q-state clock model, Phys. Rev. E **101**, 060105(R) (2020).

[42] S. Hong and D.-H. Kim, Tensor network calculation of the logarithmic correction exponent in the *XY* model, J. Phys. Soc. Jpn. **91**, 084003 (2022).

[43] G. Li, K. H. Pai, and Z.-C. Gu, Tensor-network renormalization approach to the q-state clock model, Phys. Rev. Res. **4**, 023159 (2022).

[44] F.-F. Song and G.-M. Zhang, Tensor network approach to the two-dimensional fully frustrated *XY* model and a chiral ordered phase, Phys. Rev. B **105**, 134516 (2022).

[45] T. D. Lee and C. N. Yang, Statistical theory of equations of state and phase transitions. II. Lattice gas and Ising model, Phys. Rev. **87**, 410 (1952).

[46] A. Šarlah, E. Frey, and T. Franosch, Spin models for orientational ordering of colloidal molecular crystals, Phys. Rev. E **75**, 021402 (2007).

[47] A. Patrykiejew, O. Pizio, and S. Sokolowski, Novel Phase Behavior in a Two-Dimensional Network-Forming Lattice Fluid, Phys. Rev. Lett. **83**, 3442 (1999).

[48] B. R. Brooks, R. E. Bruccoleri, B. D. Olafson, D. J. States, S. a Swaminathan, and M. Karplus, CHARMM: A program for macromolecular energy, minimization, and dynamics calculations, J. Comput. Chem. **4**, 187 (1983).

[49] S. L. Mayo, B. D. Olafson, and W. A. Goddard, DREIDING: A generic force field for molecular simulations, J. Phys. Chem. **94**, 8897 (1990).

[50] J.-H. Lii and N. L. Allinger, Directional hydrogen bonding in the MM3 force field. I, J. Phys. Org. Chem. **7**, 591 (1994).

[51] J.-H. Lii and N. L. Allinger, Directional hydrogen bonding in the MM3 force field: II, J. Comput. Chem. **19**, 1001 (1998).

[52] M. Levin and C. P. Nave, Tensor Renormalization Group Approach to Two-Dimensional Classical Lattice Models, Phys. Rev. Lett. **99**, 120601 (2007).

[53] S. S. Akimenko, G. D. Anisimova, A. I. Fadeeva, V. F. Fefelov, V. A. Gorbunov, T. R. Kayumova, A. V. Myshlyavtsev, M. D. Myshlyavtseva, and P. V. Stishenko, SUSMOST: Surface science modeling and simulation toolkit, J. Comput. Chem. **41**, 2084 (2020).

[54] D. P. Landau and K. Binder, *A Guide to Monte Carlo Simulations in Statistical Physics*, 4th ed. (Cambridge University Press, Cambridge, UK, 2015).

[55] T.-H. Vu and T. Wandlowski, CV and *in situ* STM study the adsorption behavior of benzoic acid at the electrified Au(100)| HClO₄ interface: Structure and dynamics, J. Electroanal. Chem. **776**, 40 (2016).

[56] C. Leasor, K.-H. Chen, T. Closson, and Z. Li, Revealing the structural complex of adsorption and assembly of benzoic acids at electrode–electrolyte interfaces using electrochemical scanning tunneling microscopy, J. Phys. Chem. C **123**, 13600 (2019).

[57] S. Clair, S. Pons, A. P. Seitsonen, H. Brune, K. Kern, and J. V. Barth, STM study of terephthalic acid self-assembly on Au (111): Hydrogen-bonded sheets on an inhomogeneous substrate, J. Phys. Chem. B **108**, 14585 (2004).

[58] M. Lackinger, S. Griessl, T. Markert, F. Jamitzky, and W. M. Heckl, Self-assembly of benzene−dicarboxylic acid isomers at the liquid solid interface: Steric aspects of hydrogen bonding, J. Phys. Chem. B **108**, 13652 (2004).

[59] M. E. Cañas-Ventura, F. Klappenberger, S. Clair, S. Pons, K. Kern, H. Brune, T. Strunskus, Ch. Wöll, R. Fasel, and J. V. Barth, Coexistence of one- and two-dimensional supramolecular assemblies of terephthalic acid on Pd(111) due to self-limiting deprotonation, J. Chem. Phys. **125**, 184710 (2006).

[60] T. Suzuki, T. Lutz, D. Payer, N. Lin, S. L. Tait, G. Costantini, and K. Kern, Substrate effect on supramolecular self-assembly: From semiconductors to metals, Phys. Chem. Chem. Phys. **11**, 6498 (2009).

[61] Y. Ge, H. Adler, A. Theertham, L. L. Kesmodel, and S. L. Tait, Adsorption and bonding of first layer and bilayer terephthalic acid on the Cu(100) surface by high-resolution electron energy loss spectroscopy, Langmuir **26**, 16325 (2010).

[62] R. Addou and M. Batzill, Defects and domain boundaries in self-assembled terephthalic acid (TPA) monolayers on CVD-grown graphene on Pt(111), Langmuir **29**, 6354 (2013).

[63] J. D. Fuhr, A. Carrera, N. Murillo-Quirós, L. J. Cristina, A. Cossaro, A. Verdini, L. Floreano, J. E. Gayone, and H. Ascolani, Interplay between hydrogen bonding and molecule–substrate interactions in the case of terephthalic acid molecules on Cu(001) surfaces, J. Phys. Chem. C **117**, 1287 (2013).

[64] C. Leasor, K. Goshinsky, K.-H. Chen, and Z. Li, Probing molecular nanostructures of aromatic terephthalic acids triggered by intermolecular hydrogen bonds and electrochemical potential, Langmuir **35**, 13259 (2019).

[65] A. Dmitriev, N. Lin, J. Weckesser, J. V. Barth, and K. Kern, Supramolecular assemblies of trimesic acid on a Cu(100) surface, J. Phys. Chem. B **106**, 6907 (2002).

[66] Y. Ye, W. Sun, Y. Wang, X. Shao, X. Xu, F. Cheng, J. Li, and K. Wu, A unified model: Self-assembly of trimesic acid on gold, J. Phys. Chem. C **111**, 10138 (2007).

[67] M. S. Baviloliaei and L. Diekhöner, Molecular self-assembly at nanometer scale modulated surfaces: Trimesic acid on Ag(111), Cu(111) and Ag/Cu(111), Phys. Chem. Chem. Phys. **16**, 11265 (2014).

[68] S. Griessl, M. Lackinger, M. Edelwirth, M. Hietschold, and W. M. Heckl, Self-assembled two-dimensional molecular host-guest architectures from trimesic acid, Single Mol. **3**, 25 (2002).

[69] J. M. MacLeod, J. A. Lipton-Duffin, D. Cui, S. De Feyter, and F. Rosei, Substrate effects in the supramolecular assembly of 1,3,5-benzene tricarboxylic acid on graphite and graphene, Langmuir **31**, 7016 (2015).

[70] T. Classen, M. Lingenfelder, Y. Wang, R. Chopra, C. Virojanadara, U. Starke, G. Costantini, G. Fratesi, S. Fabris, S. de Gironcoli *et al.*, Hydrogen and coordination bonding supramolecular structures of trimesic acid on Cu(110)†, J. Phys. Chem. A **111**, 12589 (2007).